Estuarine, Coastal and Shelf Science 79 (2008) 143–151

Contents lists available at ScienceDirect

Estuarine, Coastal and Shelf Science

journal homepage: www.elsevier.com/locate/ecss

A multi-scale model of the hydrodynamics of the whole Great Barrier Reef

Jonathan Lambrechts [a,*], Emmanuel Hanert [b], Eric Deleersnijder [a], Paul-Emile Bernard [a], Vincent Legat [a], Jean-François Remacle [c,a], Eric Wolanski [e,d]

[a] Université catholique de Louvain, Centre for Systems Engineering and Applied Mechanics, B-1348 Louvain-la-Neuve, Belgium
[b] The University of Reading, Department of Meteorology, Earley Gate, P.O. Box 243, Reading RG6 6BB, UK
[c] Université catholique de Louvain, Département de Génie Civil et Environmental, B-1348 Louvain-la-Neuve, Belgium
[d] Australian Institute of Marine Science (AIMS), PMB No. 3, Townsville MC, Queensland, 4810 Australia
[e] James Cook University, James Cook Drive, Townsville, Queensland 4811, Australia

ARTICLE INFO

Article history:
Received 2 October 2007
Accepted 21 March 2008
Available online 1 April 2008

Keywords:
Great Barrier Reef
hydrodynamics
shelf dynamics
finite elements
unstructured mesh
East Australian Current

ABSTRACT

An unstructured-mesh parallel hydrodynamic model of the whole Great Barrier Reef is presented. This model simultaneously simulates most scales of motion. It allows interactions between small- and large-scale processes. The depth-averaged equations of motion are discretized in space by means of a mixed finite element formulation while the time-marching procedure is based on a third order explicit Adams–Bashforth scheme. The mesh is made up of triangles. Their size and shape can be modified easily so as to resolve a wide range of scales of motion, from those of the regional flows to those of the eddies or tidal jets that develop in the vicinity of reefs and islands. The forcings are the surface wind stress, the tides and the inflow from the Coral Sea (East Australian Current, Coral Sea Coastal Current), the latter two forcings being applied along the open boundaries of the computational domain. The numerical results compare favourably with observations of both longshore currents and the local perturbations due to narrow reef passages. Comparisons are also performed with the simulations of a three-dimensional model applied to a small domain centered on Rattray Island, showing that both models produce similar horizontal flow fields. For a structured-mesh model to yield results of the same accuracy, there is no doubt that the computational cost would be much higher.

1. Introduction

The Great Barrier Reef is on the continental shelf of the Australian northeastern coastline as illustrated in Fig. 1. There are over 2500 coral reefs in a strip that is about 2600 km in length and 200 km in width. Due to recent human activities, these ecosystems deteriorate at an alarming rate. Land use contributes to the degradation of the Great Barrier Reef health and to an increased frequency and intensity of crown-of-thorns starfish infestations (Wolanski and De'ath, 2005; Richmond et al., 2007). Therefore, there is a strong need for accurate hydrodynamical simulations allowing to better understand and analyse the interactions between ecological processes and human impacts (Richmond, 1993; Veron, 1995; Birkeland, 1997; Wilkinson, 1999; Wolanski, 2001; Werner et al., 2007). Today, developing a high resolution, efficient and realistic model of the hydrodynamics of the whole Great Barrier Reef is still a difficult task in view of the complex bathymetry and topography. Taking up this challenge is the objective of the present study.

The circulation over the Great Barrier Reef shelf is mainly controlled by the complex topography, the local wind, the tidal motions and the shoreward South Equatorial Current in the western Coral Sea. On meeting the continental slope of the Great Barrier Reef, this current splits at a bifurcation point between 14° S and 18° S into the northward-flowing Coral Sea Coastal Current and the southward-flowing East Australian Current (Wolanski, 1994). These longshore currents are modulated and deviated by the wind, the tides and the topography, which can strongly deflect the mean current away from areas of high-reef density. The mean current is an essential ingredient of the ecosystem as it flushes the shelf and controls the dominant spreading direction of material emanating from reefs (Wolanski and Spagnol, 2000; Brinkman et al., 2001; Wolanski et al., 2003b; Luick et al., 2007). In other words, it controls the connectivity of reef populations as a result of the transport of water-borne larvae between reefs (Wolanski et al., 1997, 2004; Armsworth and Bode, 1999) or the transport of nutrients and pollutants by water currents (Done, 1988; Bell and Elmetri, 1995; Wolanski et al., 1999). Moreover, tidal jets and eddies occur in the wake of islands and also have a significant impact on the

* Corresponding author.
E-mail address: jonathan.lambrechts@uclouvain.be (J. Lambrechts).

0272-7714/$ – see front matter © 2008 Elsevier Ltd. All rights reserved.
doi:10.1016/j.ecss.2008.03.016

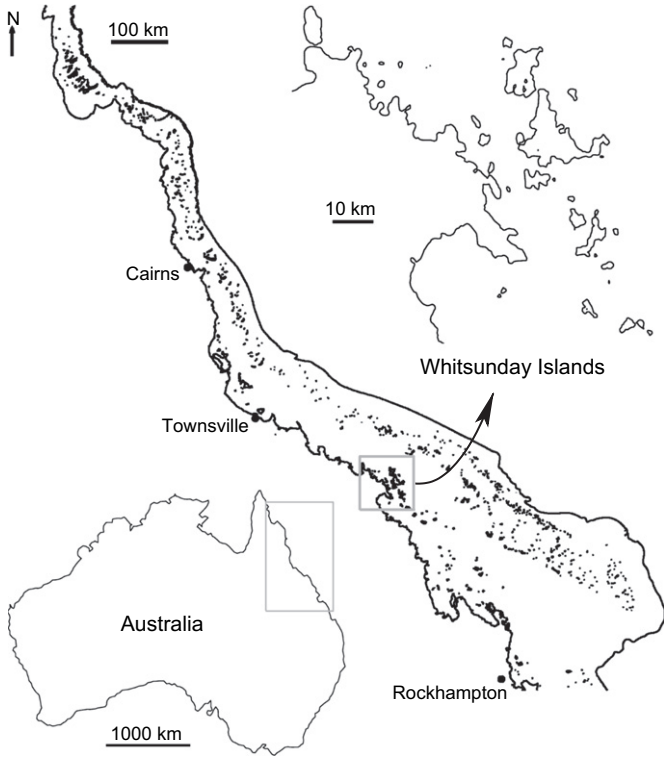

Fig. 1. Map of the whole Great Barrier Reef complex topography. The model computational domain is located between the coastline and the continental shelf break defined by the isobath of 200 m.

ecosystem. Their length scales range from about a 100 m to a few kilometres. In situ measurements, satellite imagery and numerical simulations show that those small-scale phenomena are mainly confined to the neighbourhood of small reefs, islands and passages (Hamner and Hauri, 1981; Wolanski and Hamner, 1988; Wolanski et al., 1988, 1996; Deleersnijder et al., 1992).

The above-mentioned processes occur over a wide range of space and time scales, from a few metres to hundreds of kilometres and from a few seconds to several years. It is essential to simultaneously simulate all scales of motion, because small- and large-scale processes experience significant interactions (Wolanski et al., 2003c). Clearly, a model focusing on a single phenomenon while ignoring others may lead to misleading results. However, all scales of motion cannot be reproduced by the present-day structured uniform grid models of the Great Barrier Reef. Typically, the cell size of these models is around 2000 m (King and Wolanski, 1996; Brinkman et al., 2001), i.e. larger than the characteristic sizes of a whole class of biological and hydrodynamic processes. For a uniform grid model to reproduce small-scale processes such as eddies and tidal jets, the computational cost is likely to be crippling. This is why variable resolution is needed. This could be achieved by having recourse to nested grids (Spall and Holland, 1991; Fox and Maskell, 1995). However, the regions where enhanced resolution would be needed are so numerous in the Great Barrier that this approach is unlikely to be feasible. This is why the parallel model developed herein is based on an unstructured, variable-resolution mesh that offers a very strong geometrical flexibility (Pietrzak et al., 2005; Walters, 2005; Legrand et al., 2006).

2. Unstructured-mesh hydrodynamic model

Using the same mathematical framework as the previous structured grid models (Wolanski et al., 1996; Brinkman et al., 2001), a depth-averaged barotropic model is implemented to compute the mean horizontal vector and the sea surface elevation. Unlike previous models, the equations are here discretized on a fully unstructured mesh of approximately 850,000 triangular elements depicted in Fig. 2. The mesh resolution ranges from 150 m along tiny islands to 10 km in open areas: high resolution is introduced only where the flow features require it. The local resolution is often quite finer than the grid cell of 2 km used in the simulations of Brinkman et al. (2001).

Paradoxically, the ability of the grid to represent the reef scales leads one to question the use of a depth-averaged barotropic model. When the grid size is larger than 1 km, the shallow water equations can be used to simulate the flow because at those length scales the shelf water is generally well mixed throughout the year and the flow is primarily horizontal, as pointed by Brinkman et al. (2001) and Wolanski (1994). At the reef scale, three-dimensional features, like the eddies in the wake of islands, can no longer be neglected. Both experimental observations and numerical simulations reveal that these eddies have a full three-dimensional structure that creates some strong upwelling in their centre and even stronger downwelling along their edges (Wolanski, 1994; White and Deleersnijder, 2007). Moreover, if the element size is of the order of the local water depth, non-hydrostatic effects can no longer be neglected and a hierarchical modelling should be introduced. Such an approach is a very ambitious task that would require numerous validations, comparisons and tailored parameterizations (Wolanski et al., 1996). It must also be pointed out that several authors claim that two-dimensional models produce very accurate and physically relevant horizontal currents even for the tidal circulation in island's wakes or headland eddies (Falconer et al., 1986; Pattiaratchi et al., 1986). This is because the depth is small and the water column is well mixed. The present model may be considered a first step towards a much more sophisticated simulation tool in which the equations and numerical methods would locally depend on the mesh size. The model domain covers most of the Great Barrier Reef from the Great Keppel Island in the south to the Forbes Island in the north. This computational domain is almost twice as large as that of Brinkman et al. (2001).

The continuity and horizontal momentum equations read

$$\begin{cases} \dfrac{\partial \eta}{\partial t} + \dfrac{\partial (Hu)}{\partial x} + \dfrac{\partial (Hv)}{\partial y} = 0, \\ \dfrac{\partial u}{\partial t} + u\dfrac{\partial u}{\partial x} + v\dfrac{\partial u}{\partial y} - fv + g\dfrac{\partial \eta}{\partial x} = \dfrac{1}{H}\left(\dfrac{\partial}{\partial x}\left(\nu H \dfrac{\partial u}{\partial x}\right) + \dfrac{\partial}{\partial y}\left(\nu H \dfrac{\partial u}{\partial y}\right)\right) + \dfrac{\tau_x}{\rho H} - \dfrac{g\|\mathbf{u}\|}{C^2 H}u, \\ \dfrac{\partial v}{\partial t} + u\dfrac{\partial v}{\partial x} + v\dfrac{\partial v}{\partial y} + fu + g\dfrac{\partial \eta}{\partial y} = \dfrac{1}{H}\left(\dfrac{\partial}{\partial x}\left(\nu H \dfrac{\partial v}{\partial x}\right) + \dfrac{\partial}{\partial y}\left(\nu H \dfrac{\partial v}{\partial y}\right)\right) + \dfrac{\tau_y}{\rho H} - \dfrac{g\|\mathbf{u}\|}{C^2 H}v, \end{cases} \tag{1}$$

where η, u and v are the sea surface elevation (positive upwards) and the horizontal velocity components. The actual water depth is $H = h + \eta$, where h is the reference water depth below the mean sea level. The Coriolis parameter, the gravitational acceleration, the horizontal eddy viscosity, the mean water density are respectively denoted f, g, ν and ρ. At the surface of the sea, the wind stress is $\boldsymbol{\tau} = (\tau_x, \tau_u)$. The bottom stress is parametrized as a quadratic expression, $(g/C^2H)\|\mathbf{u}\|\mathbf{u}$, where the Chezy coefficient is $C = H^{(1/6)}/n$, n being the Manning coefficient. The system of partial differential equation above has to be supplemented with mathematically relevant initial and boundary conditions in order to define a well-posed boundary value problem. It is noteworthy that the influence of the initial conditions becomes negligible after some time, due to exchanges with the Coral Sea as well as frictional and viscous dissipations.

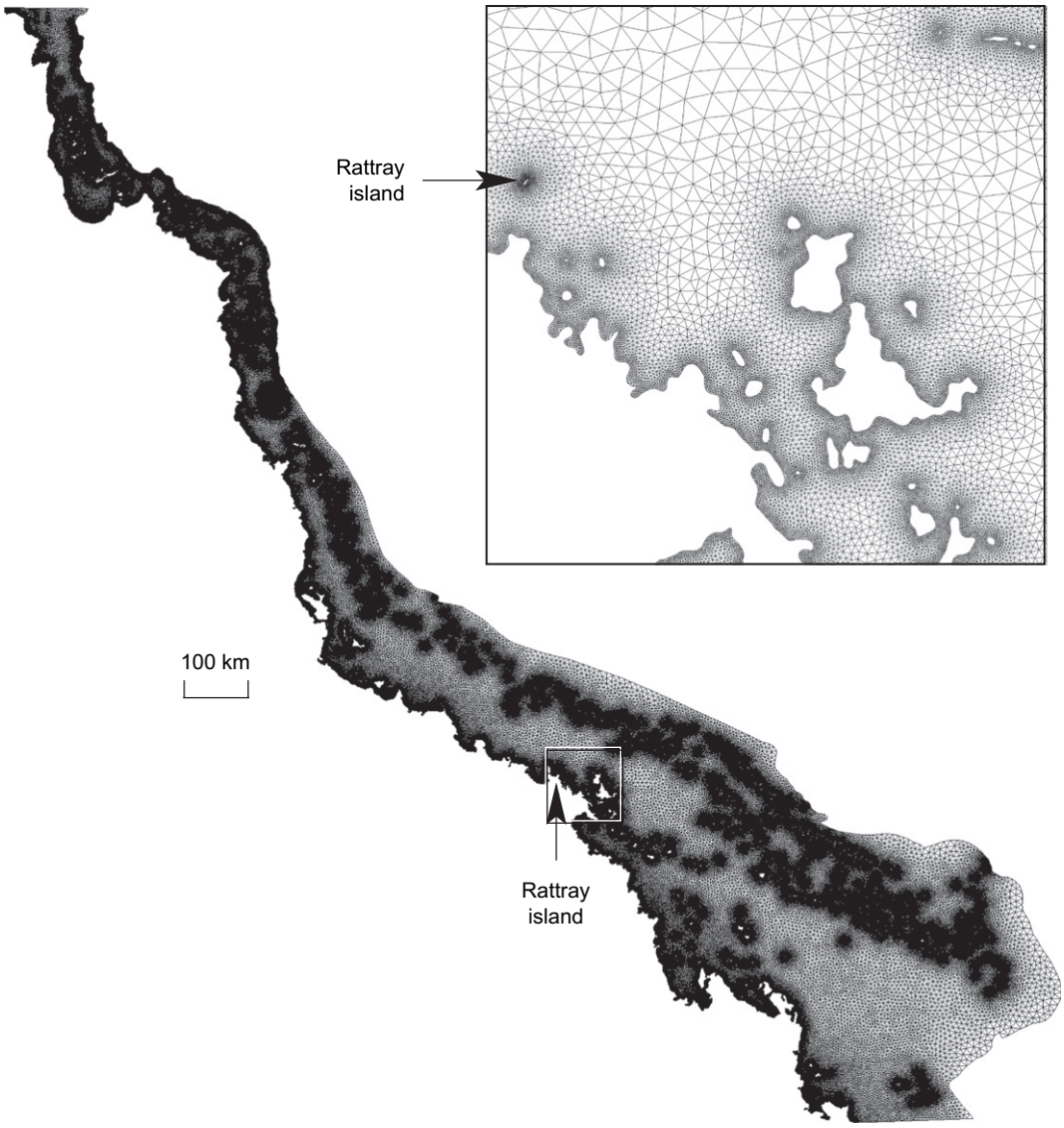

Fig. 2. Mesh of 850,843 triangles of sizes comprized between 150 m and 10 km. The number of elements and nodes are 850,843 and 500,142, respectively.

A zero mass flux and a tangential momentum flux proportional to the mean tangential velocity are imposed along the impermeable boundaries

$$\begin{cases} u_n = 0, \\ \nu \dfrac{\partial u_s}{\partial n} - \alpha u_s = 0, \end{cases} \tag{2}$$

where the indices s and n are associated with the direction tangential and normal to the boundary, respectively, u_s and u_n are the components of the depth-averaged horizontal velocity along those directions. The unresolved boundary layer along the coasts is parametrized by an empirical and purely phenomenological partial slip condition (Deleersnijder, 1996). Designing conditions to be imposed on the open part of the boundary is rather delicate. As mentioned by Blayo and Debreu (2005), a large number of alternative conditions can be used to introduce the tides and the low-frequency currents at an open boundary. A usual approach would be to specify the elevation as a function of position and time. However, it was observed by Flather (1976) that such an approach is unsatisfactory near the shelf edge. It seems that the best option is to prescribe a relationship between elevation and velocity in terms of incoming characteristic variables (Reid and Bodine, 1968; Blayo and Debreu, 2005) and to supplement it by imposing a zero depth-averaged shear stress

$$\begin{cases} u_n - \sqrt{\dfrac{g}{H}}\eta = \zeta, \\ \nu \dfrac{\partial u_s}{\partial n} = 0. \end{cases} \tag{3}$$

where the function ζ is derived from external data. For the Great Barrier Reef, measurements of the sea surface elevation at some locations in the Coral Sea can be used to force the tides and the mean currents. By assuming a zero normal transport gradient on the boundary, the normal velocity outside the domain of interest may be obtained by extrapolation from that computed inside the computational domain. These conditions appear to be satisfactory, mainly because they prevent numerical instabilities from developing.

An approximate solution of the partial differential equations under the boundary conditions specified above is obtained by using the finite element method, as it can handle unstructured grids, contrary to the finite difference method. A linear piecewise

discretization is used for both elevation and velocity fields. In order to avoid any spurious numerical modes, we use a discontinuous velocity together with a continuous piecewise linear elevation. Such an approximation is known as P_1^{NC}–P_1. Details about the mathematical analysis and numerical validation of this element for the shallow water equations are given by Hua and Thomasset (1984), Hanert et al. (2004, 2005), Le Roux (2005). With this scheme, special care is needed for implementing the boundary conditions. We weakly impose boundary conditions in terms of the characteristic variables of the first-order hyperbolic terms of the equations. Regarding the time-marching procedure, a third order explicit Adams–Bashforth integration scheme is selected. It is only conditionally stable but appears to be a quite good compromise between simplicity, efficiency and accuracy. In order to take advantage of parallel computing, the mesh is partitioned into subdomains attributed to each of the processors of a parallel cluster. The mesh partitioning is designed to uniformly distribute the computing charge and minimise the communications. The parallel speed-up is defined as the ratio of the computing time for the model running on one processor to the time needed to carry out a run on several processors. If the communication time is negligible and the computing load is equally distributed, the speed-up must be equal to the number of processors. This ideal, theoretical value is almost obtained by the present model, as illustrated in Fig. 3.

3. Selection of the physical and the numerical parameters

The first ingredient of the numerical calculations is the design of the unstructured grid. Firstly, it is critical to accurately represent the Australian coastline, the open boundaries and all relevant islands. Secondly, we define the mesh resolution from the physical processes that should be simulated. The mesh is obtained by means of the `gmsh` software. The resolution of the mesh in Fig. 2 depends on two *a priori* criteria.

- The local mesh size has to be proportional to the square root of the water depth in order to obtain the same Courant–Friedrichs–Lewy condition (CFL condition) for the gravity waves over the whole domain. In other words, the element size is adjusted in such a way that the external inertia-gravity waves travel over the same fraction of each element for a given time interval (Henry and Walters, 1993; Foreman et al., 1995; Jarosz et al., 2005; Walters, 2005).
- The local mesh size depends on the distance to islands and reefs in order to cluster mesh nodes in regions where small-scale processes are likely to take place. The mesh is refined even more in the vicinity of islands where eddies and tidal jets can be expected.

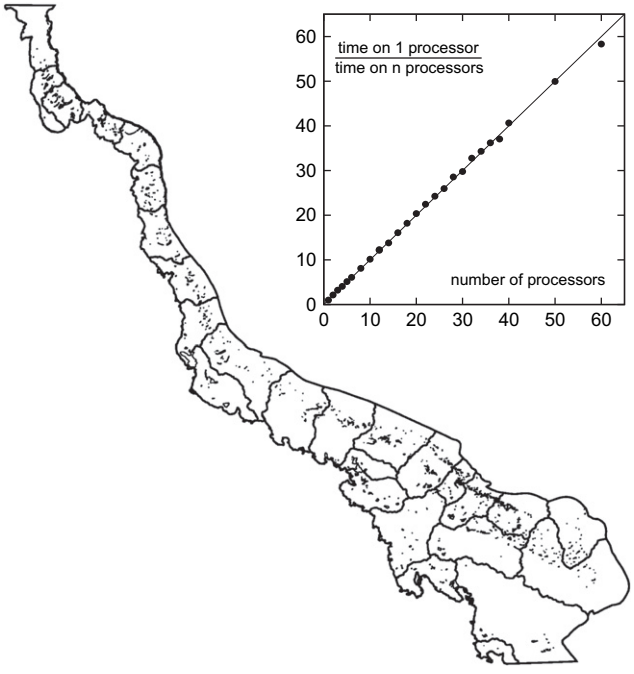

Fig. 3. Partition of the mesh into 25 sub-domains for parallel computing. The speed-up almost exactly follows the ideal line.

Both criteria are blended together so as to have a high resolution in the vicinity of reefs and islands and a resolution depending only on the bathymetry elsewhere (Legrand et al., 2006). A more ambitious strategy would be to introduce adaptive meshes. The element size could be dynamically adjusted using an *a posteriori* error estimator from the numerical discontinuities in the solution at the element interfaces (Bernard et al., 2007). A quasi-optimal mesh could then be derived for a whole simulation. Even if it may appear attractive, we think that dynamically adapting the mesh during the time integration would not provide a significant improvement as most refinement regions can be easily predicted *a priori*. The second issue is to define the parameters to represent subgrid effects. To incorporate unresolved turbulent features and boundary layers along the coastlines and islands, we use a Smagorinsky's parametrization (Smagorinsky, 1963). The value of the horizontal eddy kinematic viscosity ν depends on the local mesh size Δ and the flow structure. The parameter controlling the friction on coast and islands, α is constant

$$\nu = (0.1\Delta)^2\sqrt{2\left(\frac{\partial u}{\partial x}\right)^2+2\left(\frac{\partial v}{\partial y}\right)^2+\left(\frac{\partial u}{\partial y}+\frac{\partial v}{\partial x}\right)^2}, \qquad \alpha = 2.5\times10^{-3}\ \mathrm{m/s}. \tag{4}$$

Finally, the value of the Manning coefficient is taken from (King and Wolanski, 1996) $n = 2.5\times10^{-2}\ \mathrm{m}^{-1/3}\mathrm{s}$.

The external forcings of the hydrodynamics of the Great Barrier Reef are the wind, the adjacent Coral Sea circulation and the tides. Wind data are extracted from the NCEP reanalysis data provided by the NOAA/OAR/ESRL PSD, Boulder, Colorado, USA (Kalnay et al., 1996). The stress acting on the sea due to the wind is modelled by using the parametrization proposed by (Smith and Banke, 1975)

$$\boldsymbol{\tau} = \underbrace{10^{-3}\left(0.630\|\mathbf{v}_w\| + 0.066\|\mathbf{v}_w\|^2\right)}_{C(\mathbf{v}_w)}\mathbf{v}_w, \tag{5}$$

where $\mathbf{v}_w$ is the surface wind velocity in m/s and $C(\mathbf{v}_w)$ is a scaling parameter expressed in $\mathrm{kg\,m^{-2}\,s^{-1}}$. To incorporate the effect of the East Australian Current, the Coral Sea Coastal Current and the tides coming from the Coral Sea, we have to specify the elevation $\eta_{\mathrm{sea}}(x,y,t)$ on the open-sea part of the boundary. The measurements of the elevations at several locations accurately provide the tidal dynamics, but the global currents effect is largely covered by noise and long-term fluctuations. Therefore, we prescribe the elevation at the open-sea boundary as follows:

$$\eta(x,y,t) = \overline{\eta}(x,y) + \eta'(x,y,t) \tag{6}$$

where $\eta'(x,y,t)$ is the temporal variations of the measurement of the sea level in the Coral Sea and $\overline{\eta}(x,y)$ is a steady-state elevation imposed to obtain the East Australian Current and the Coral Sea Coastal Current in the computational domain in a time-averaged sense. The temporal variations of the tidal elevation on the north-western, eastern and south-eastern open boundaries are obtained

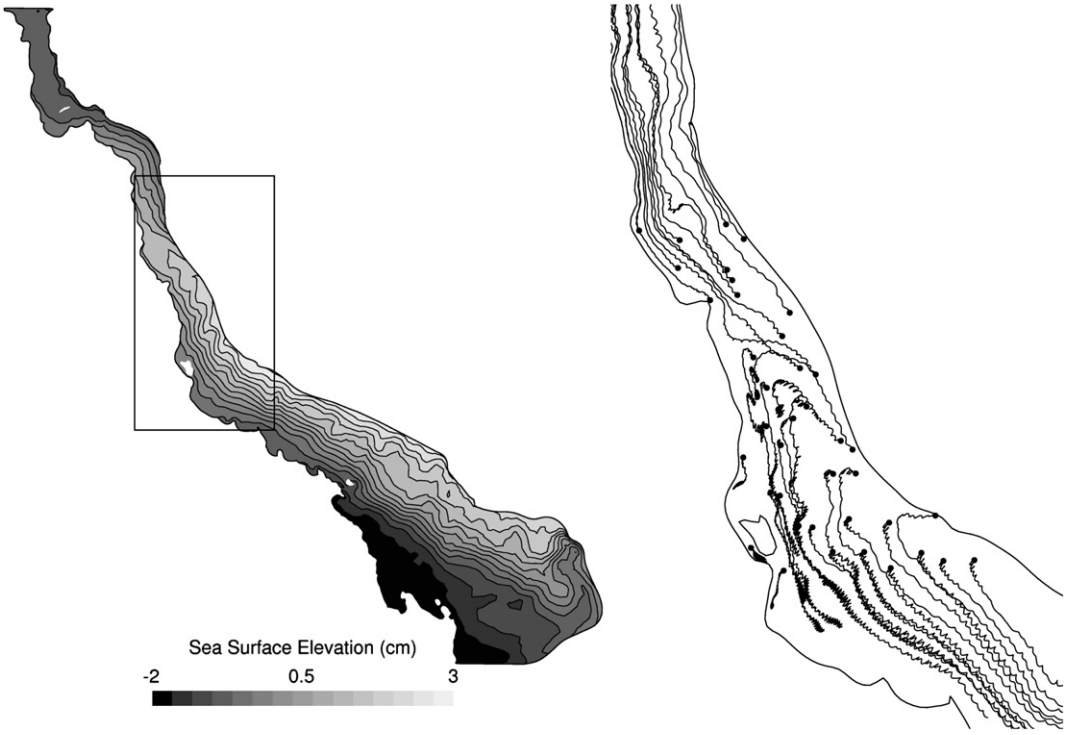

Fig. 4. On the left-hand side, mean sea surface elevation $\overline{\eta}(x)$ obtained from the auxiliary steady-state problem and prescribed on the open-sea boundaries to enforce the low-frequency currents. On the right-hand side, Lagrangian particles' trajectories illustrating both the tidal motions and the large-scale currents.

by a linear interpolation from 15 measurement sites where the National Australian Time Tables provide the elevation and phase shift of the 12 principal tidal constituents. As the amplitude of the temporal variations is larger than the variations of $\overline{\eta}(x,y)$, it appears unwise to have confidence is the constant part of the data. Moreover, large-scale features also are included in those data and render them incompatible with the assumption of a spatially established flow along the boundary.

In order to circumvent this incompatibility, we use an auxiliary steady-state problem to identify the suitable form of the function $\overline{\eta}(x,y)$. This auxiliary problem consists in using the East Australian Current and the Coral Sea Coastal Current as the unique forcing in terms of velocity along the whole boundary. Opposite flows are induced by prescribing the longshore velocity at the upper and lower parts of the open-sea boundary. In an intermediate neutral area, we define a zone of incoming cross-shore current separating them. Dividing the boundary in such a way is justified from the observations (Brinkman et al., 2001). When a steady state is reached, the surface elevation on the boundaries is considered as a good candidate to enforce both currents. Left-hand side panel in Fig. 4 shows contour lines of the mean sea surface elevation $\overline{\eta}(x)$ obtained from the auxiliary steady-state problem and used as prescribed mean elevation at the open boundary. Due to the Coriolis force, the elevation essentially varies in the longshore direction in the central part of the Great Barrier Reef while it is in the cross-shore direction elsewhere. On the right-hand side, trajectories of Lagrangian particles are displayed in the box drawn on the left-hand side panel. Both tidal motions and large-scale current effects can be easily identified. The separation of the oceanic inflow into two branches occurs at a location in accordance with field data.

As the problem is non-linear and as the tidal motions generate a larger amount of dissipation, it is necessary to multiply the steady-state solution to get the adequate $\overline{\eta}(x,y)$ by a scalar factor in order to obtain the correct mean flow when the time average is performed. Typically, this factor ranges from 2 to 3. It must be pointed out that this approach is a purely phenomenological way to close the problem and to enforce large-scale flow features in the computational domain. This approach is the least stringent way to enforce the global currents and seems to be less invasive than the strategy proposed by Brinkman et al. (2001).

4. Discussion

Low-frequency, longshore currents are well predicted by the model, as shown in Fig. 4 where the trajectories of Lagrangian particles illustrate both the tidal variations and the long-term flow. More critical is the model's ability to represent a broad range of

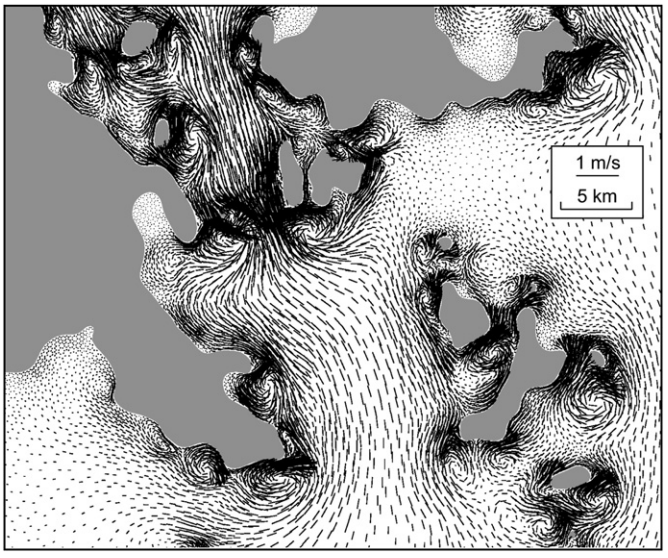

Fig. 5. Sticky water in the southern part of the Withsundays Islands Archipelago (20°21′ S 149°00′ E).

scales: let us just cite the tide as a propagating wave over the shelf described by Wolanski and Hamner (1988), the eddies and tidal jets created by the topography. The interaction of the tidal currents with many islands and reefs acting together generates macro-turbulence which makes the regions of high-reef density less permeable to low-frequency currents at spring tides than at neap-tides. This large-scale sticky water effect (Wolanski and Spagnol, 2000; Spagnol et al., 2001) illustrates a feedback process whereby the small-scale processes influence the large-scale flows, as discussed by Wolanski et al. (2003a) for one specific area. Those secondary flows, illustrated in Fig. 5, are widespread throughout the Great Barrier Reef both in coastal waters as well as in the Great Barrier Reef matrix. This has important biological implications because the connectivity between various areas will vary according to the reef and island density.

In order to estimate the accuracy of the model in modelling the tidal waves propagation, we compare the calculated sea surface elevation with observations at five sites widespread on the continental shelf away from boundaries. Numerical results and observations are shown in Fig. 6. We see a good agreement between the predicted and observed elevations, both in terms of amplitude and phase shift.

We compare the predicted results with some small-scale three-dimensional calculations performed by White and Deleersnijder (2007) and White and Wolanski (2008) around Rattray Island. In their calculations, White and Deleersnijder (2007) used a rectangular computational domain of approximately 100 km^2 and obtained results that compare favourably with measurements performed by Wolanski et al. (1984). Fig. 7 shows the eddies past Rattray Island simulated by the present two-dimensional model and the aforementioned three-dimensional model. Though the resolution of the former model is coarser, the eddies simulated by both models are quite similar, pointing to the ability of the two-dimensional to represent small-scale flow features. Presumably, tidal jets are also well simulated. They occur when the flow is accelerated through narrow reef passages. The resulting unstable jet produces a pair of eddies at the outflow (Fig. 8). These mushroom shaped circulation patterns, well predicted when the flow is accelerated between both islands, have been observed in the field by Wolanski (1994). To avoid smearing

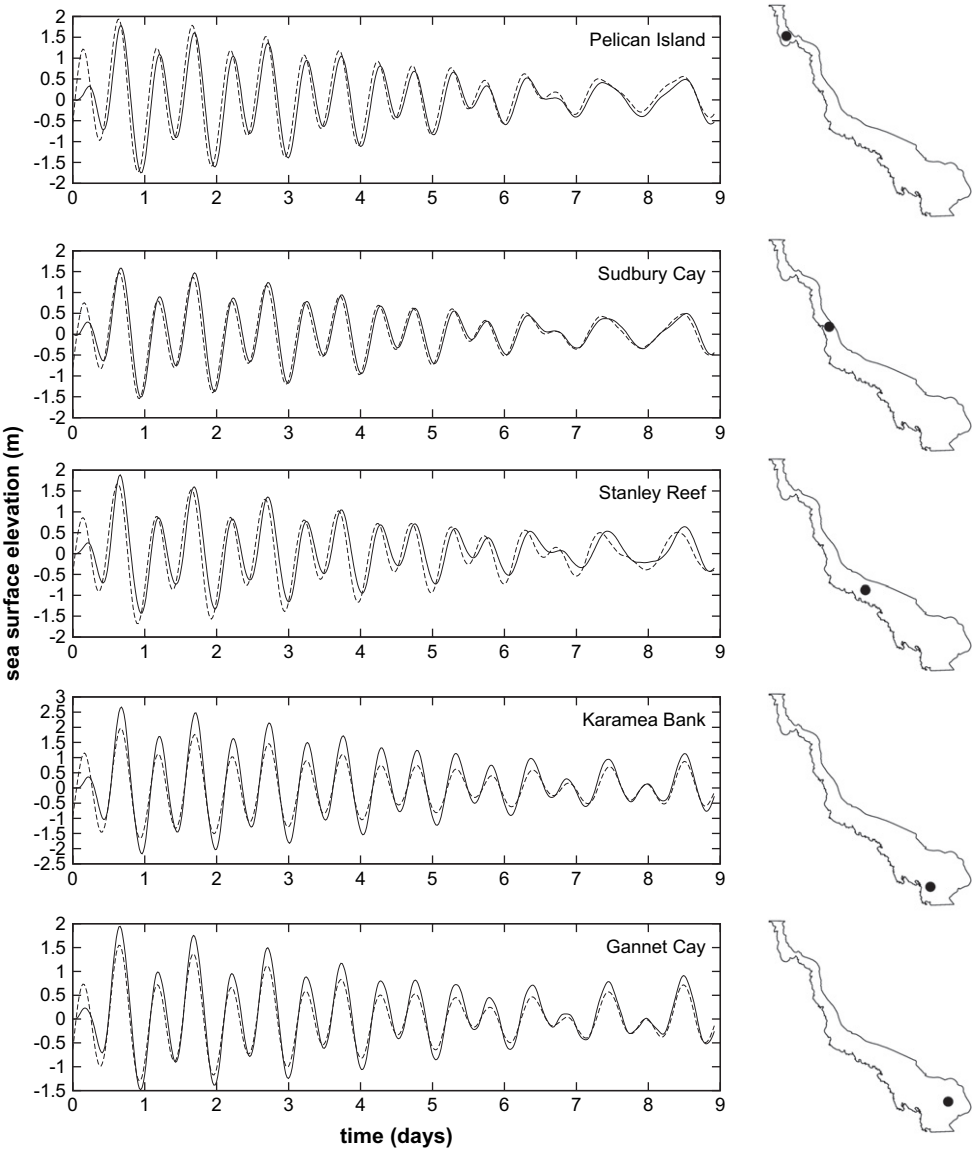

Fig. 6. Series of observed and predicted sea surface elevation at measurement sites spread over the GBR. Measured elevations are represented with dashed lines, while the predictions are given in a continuous line.

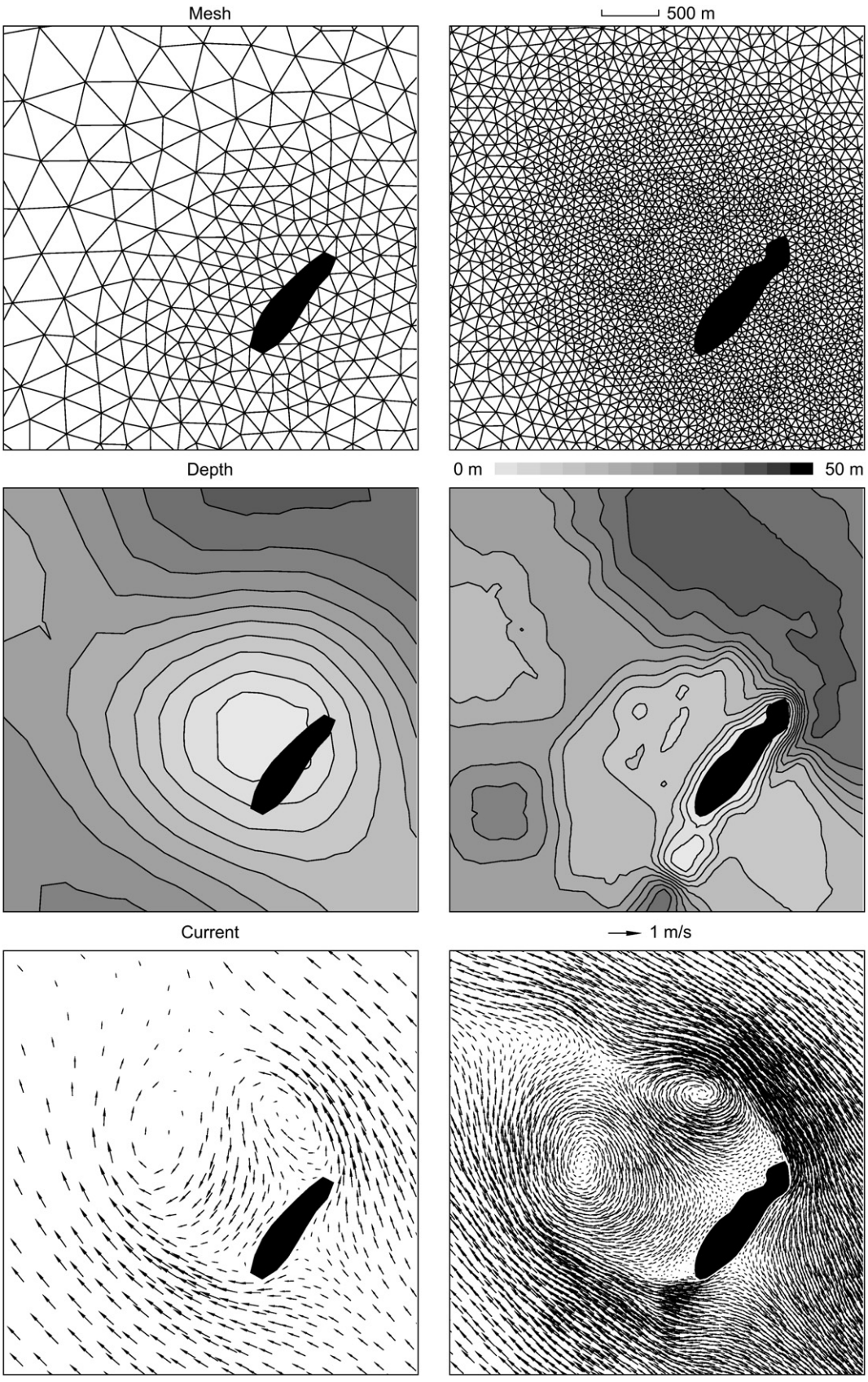

Fig. 7. Close-up views of meshes, bathymetry and eddies at a given time from our global model and the three-dimensional small-scale calculations of White and Deleersnijder (2007) are presented on the left- and right-hand sides, respectively.

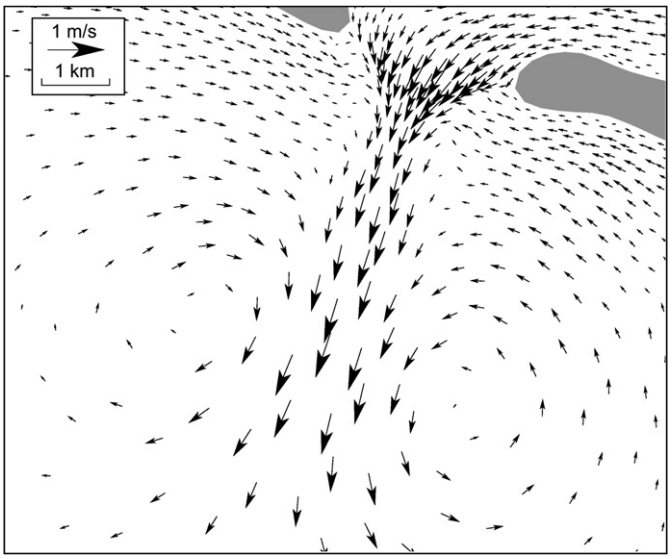

Fig. 8. Tidal jets and eddies due to the interaction of the flow with the topography near the open-sea boundary (14°17′ S 145°08′ E).

out these flow features, the diffusion induced by the numerical scheme must be kept as small as possible. In our calculations, this numerical viscosity is always smaller than the parametrized physical viscosity.

Even if small-scales features are well predicted by the model, we must emphasize that the hierarchical adaptive grid does not correspond to a hierarchical mathematical modelling. Basically, we still consider the same shallow water equations when the grid refinement implies that the non-hydrostatic processes might not be negligible. A careful analysis of the subgrid closure modelling and parametrization is certainly the next step of our work. However, our simulations show that the complex topography of the Great Barrier Reef introduces major spatial and temporal variability in the circulation of this region, as mentioned by King (1992), King and Wolanski (1996), Wolanski and Spagnol (2000) and Brinkman et al. (2001). Even the flow around a single coral reef is also taking place over a broad range of scales (Monismith, 2007). The physics involved undergoes huge changes when going from the size of a coral colony (mm to cm) to the whole reef scale (100 m–1 km). Of particular interest is the boundary layer flow over the reefs, which is mainly influenced by the complex and porous geometry of the reefs. The resulting drag from reefs is much larger than the drag from muddy or sandy seabeds (Roberts et al., 1975; Lugo Fernandez et al., 1998). Therefore, incorporating variable bottom friction coefficient and adapting the subgrid viscosity model could render the model more realistic as a predictive tool for ecological applications. But even if the present work has to be considered as a first attempt towards a three-dimensional high-resolution model of the whole Great Barrier Reef, it now appears possible to broaden the range of scales simulated by a single model. A large number of small-scale features could be well represented and used to better understand the complex flow dynamics of the Reef. This work also shows that the variability of the topographical details strongly influences the magnitude of the small-scales features and not only the locations of exchange between the Coral Sea and the Great Barrier Reef.

Acknowledgements

Eric Deleersnijder is a Research Associate with the Belgian National Fund for Scientific Research (FNRS). The present study was carried out within the scope of the project "A second-generation model of the ocean system", which is funded by the *Communauté Française de Belgique*, as *Actions de Recherche Concertées*, under contract ARC 04/09-316. This work is a contribution to the development of SLIM, the Second-generation Louvain-la-Neuve Ice-ocean Model. Emmanuel Hanert thanks the Nuffield Foundation for a newly appointed lecturer award.

References

Armsworth, P., Bode, L., 1999. The consequences of non-passive advection and directed motion for population dynamics. Proceedings of the Royal Society A: Mathematical, Physical and Engineering Sciences 455, 4045–4060.
Bell, R., Elmetri, I., 1995. Ecological indicators of large-scale eutrophication in the Great Barrier Reef lagoon. Ambio 24, 208–215.
Bernard, P.-E., Chevaugeon, N., Legat, V., Deleersnijder, E., Remacle, J.-F., 2007. High-order *h*-adaptive discontinuous Galerkin methods for ocean modeling. Ocean Dynamics 57, 109–121.
Birkeland, C.E., 1997. Life and Death of Coral Reefs. Chapman and Hall, New York.
Blayo, E., Debreu, L., 2005. Revisiting open boundary conditions from the point of view of characteristic variables. Ocean Modelling 9, 231–252.
Brinkman, R., Wolanski, E., Deleersnijder, E., McAllister, F., Skirving, W., 2001. Oceanic inflow from the Coral Sea into the Great Barrier Reef. Estuarine, Coastal and Shelf Science 54, 655–668.
Deleersnijder, E., 1996. On the numerical treatment of a lateral boundary layer in a shallow sea model. Journal of Marine Systems 8, 107–117.
Deleersnijder, E., Norro, A., Wolanski, E., 1992. A three-dimensional model of the water circulation around an island in shallow water. Continental Shelf Research 12, 891–906.
Done, T., 1988. Simulations of the recovery of pre-disturbance size structure in populations of *Porites* spp. damaged by crown-of-thorns starfish. Marine Biology 100, 51–61.
Falconer, R.A., Wolanski, E., Mardapitta-Hadjipandeli, 1986. Modeling tidal circulation in an island's wake. Journal of Waterway, Port, Coastal and Ocean Engineering 112 (2).
Flather, R.A., 1976. A tidal model of the north-west European continental shelf. Mémoires de la Société Royale des Sciences de Liège 6 (10), 141–164.
Foreman, M., Walters, R., Henry, R., Keller, C., Dolling, A., 1995. A tidal model for eastern Juan de Fuca Strait and the southern Strait of Georgia. Journal of Geophysical Research 100 (C1), 721–740.
Fox, A.D., Maskell, S.K., 1995. Two-way interactive nesting of primitive equation ocean models with topography. Journal of Physical Oceanography 25, 2977–2996.
Hamner, W., Hauri, I., 1981. Effect of island mass: water flow and plankton pattern around a reef in the Great Barrier Reef lagoon. Limnology and Oceanography 26, 1084–1102.
Hanert, E., Le Roux, D.Y., Legat, V., Deleersnijder, E., 2004. Advection schemes for unstructured grid ocean modelling. Ocean Modelling 7, 39–58. doi:10.1016/S1463-5003(03)00029-5.
Hanert, E., Le Roux, D.Y., Legat, V., Deleersnijder, E., 2005. An efficient Eulerian finite element method for the shallow water equations. Ocean Modelling 10, 115–136. doi:10.1016/j.ocemod.2004.06.006.
Henry, R., Walters, R., 1993. Geometrically based, automatic generator for irregular networks. Communications in Numerical Methods in Engineering 9, 555–566.
Hua, B.L., Thomasset, F., 1984. A noise-free finite element scheme for the two-layer shallow water equations. Tellus 36A, 157–165.
Jarosz, E., Blain, C., Murray, S., Inoue, M., 2005. Bab el Mandab Straits – numerical simulations. Continental Shelf Research 25, 1225–1247.
Kalnay, E., Kanamitsu, M., Kistler, R., Collins, W., Deaven, D., Gandin, L., Iredell, M., Saha, S., White, G., Woollen, J., Zhu, Y., Leetmaa, A., Reynolds, B., Chelliah, M., Ebisuzaki, W., Higgins, W., Janowiak, J., Mo, K.C., Ropelewski, C., Wang, J., Jenne, R., Joseph, D., 1996. The NCEP/NCAR 40-year reanalysis project. Bulletin of the American Meteorological Society 77, 437–470.
King, B., 1992. A predictive model of the currents in Cleveland Bay. In: Estuarine and Coastal Modeling. American Society of Civil Engineers, New York.
King, B.A., Wolanski, E., 1996. Tidal current variability in the central Great Barrier Reef. Journal of Marine Systems 9, 187–202.
Le Roux, D.Y., 2005. Dispersion relation analysis of the P_1^{IC}–P_1 finite-element pair in shallow-water models. SIAM Journal of Scientific Computing 27, 394–414. doi:10.1137/030602435.
Legrand, S., Deleersnijder, E., Hanert, E., Legat, V., Wolanski, E., 2006. High-resolution, unstructured meshes for hydrodynamic models of the Great Barrier Reef, Australia. Estuarine, Coastal and Shelf Science 68, 36–46.
Lugo Fernandez, A., Roberts, H.H., Wiseman, W.J., Carter, B.L., 1998. Water level and currents of tidal and infragravity periods at Tague Reef, St. Croix (USVI). Coral Reefs 17, 343–349.
Luick, J.L., Mason, L., Hardy, T., Furnas, M.J., 2007. Circulation in the Great Barrier Reef lagoon using numerical tracers and in situ data. Continental Shelf Research 27, 757–778.
Monismith, S.G., 2007. Hydrodynamics of coral reefs. Annual Review of Fluid Mechanics 39, 37–55.
Pattiaratchi, C., James, A., Collins, M., 1986. Island wakes and headland eddies: a comparison between remotely sensed data and laboratory experiments. Journal of Geophysical Research 92, 783–794.

Pietrzak, J., Deleersnijder, E., Schroeter, J.E., 2005. The second international workshop on unstructured mesh numerical modelling of coastal, shelf and ocean flows. Ocean Modelling 10, 1–252 (special issue).
Reid, R.O., Bodine, B.R., 1968. Numerical model for storms surges in Galveston Bay. American Society of Civil Engineers. Journal of Waterways, Harbors and Coastal Engineering Division 94, 33–57.
Richmond, R., Teina, R., Golbuu, Y., Victor, S., Idechong, N., Davis, G., Kotska, W., Neth, L., Hamnett, M., Wolanski, E., 2007. Watersheds and coral reefs: conservation science, policy and implementation. Bioscience 57 (7), 598–607.
Richmond, R.H., 1993. Coral reefs: present problems and future concerns resulting from anthropogenic disturbance. American Zoologist 33, 54–57.
Roberts, H.H., Murray, S.P., Suhayda, J.H., 1975. Physical process in a fringing reef system. Journal of Marine Research 33, 233–260.
Smagorinsky, J., 1963. General circulation experiments with the primitive equations. Monthly Weather Review 91, 99–164.
Smith, S.D., Banke, E.G., 1975. Variation of the sea surface drag coefficient with wind speed. Quarterly Journal of the Royal Meteorological Society 101, 665–673.
Spagnol, S., Wolanski, E., Deleersnijder, E., 2001. Steering by coral reef assemblages. In: Wolanski, E. (Ed.), Oceanographic Processes of Coral Reefs: Physical and Biological Links in the Great Barrier Reef. CRC Press, Boca Raton, Florida, pp. 231–236.
Spall, M.A., Holland, W.R., 1991. A nested primitive equation model for oceanic applications. Journal of Physical Oceanography 21, 205–220.
Veron, J.E.N., 1995. Corals in Space and Time. University of New South Wales Press, Sidney, 321 pp.
Walters, R., 2005. Coastal ocean models: two useful finite element methods. Continental Shelf Research 25, 775–793.
Werner, F., Cower, R., Paris, C., 2007. Coupled biological and physical models: present capabilities and necessary developments for future studies of population connectivity. Oceanography 20 (3), 54–69.
White, L., Deleersnijder, E., 2007. Diagnoses of vertical transport in a three-dimensional finite element model of the tidal circulation around an island. Estuarine, Coastal and Shelf Science 74, 655–669.
White, L., Wolanski, E., 2008. Flow separation and vertical motions in a tidal flow interacting with a shallow-water island. Estuarine. Coastal and Shelf Science 77 (3), 457–466.
Wilkinson, C.R., 1999. Global and local threats to coral reef functioning and existence: review and predictions. Marine and Freshwater Research 50, 867–878.
Wolanski, E., 1994. Physical Oceanographic Processes of the Great Barrier Reef. CRC Press, Boca Raton, Florida, 194 pp.
Wolanski, E., 2001. Oceanographic Processes of Coral Reefs. Physical and Biological Links in the Great Barrier Reef. CRC Press, Boca Raton, Florida, 356 pp.
Wolanski, E., Asaeda, T., Tanaka, T., Deleersnijder, E., 1996. Three-dimensional island wakes in the field, laboratory and numerical codes. Continental Shelf Research 16, 1437–1452.
Wolanski, E., Brinkmann, R., Spagnol, S., McAllister, F., Skirving, C.S.W., Deleersnijder, E., 2003a. Merging scales in models of water circulation: perspectives from the Great Barrier Reef. In: Lakhan, V. (Ed.), Advances in Coastal Modeling. Elsevier, pp. 411–429.
Wolanski, E., Marshall, K., Spagnol, S., 2003b. Nepheloid layer dynamics in coastal waters of the Great Barrier Reef, Australia. Journal of Coastal Research 19, 748–752.
Wolanski, E., Richmond, R., Davis, G., Deleersnijder, E., Leben, R., 2003c. Eddies around Guam, an island in the Mariana Islands group. Continental Shelf Research 23, 991–1003.
Wolanski, E., De'ath, G., 2005. Predicting the impact of present and future human land-use on the Great Barrier Reef. Estuarine, Coastal and Shelf Science 64, 504–508.
Wolanski, E., Doherty, P., Carleton, J., 1997. Directional swimming of fish larvae determines connectivity of fish populations on the Great Barrier Reef. Naturwissenschaften 84, 262–268.
Wolanski, E., Drew, E., Abel, K., O'Brien, J., 1988. Tidal jets, nutrient upwelling and their influence on the productivity of the algal Halimeda in the ribbon reefs, Great Barrier Reef. Estuarine, Coastal and Shelf Science 26, 169–201.
Wolanski, E., Hamner, W.M., 1988. Topographically controlled fronts in the ocean and their biological influence. Science 241, 177–181.
Wolanski, E., Imberger, J., Heron, M.L., 1984. Island wakes in shallow coastal waters. Journal of Geophysical Research 20, 10553–10569.
Wolanski, E., King, B., Spagnol, S., 1999. Perspectives in Integrated Coastal Zone Management. Springer-Verlag, Berlin, pp. 129–141.
Wolanski, E., Spagnol, S., 2000. Sticky waters in the Great Barrier Reef. Estuarine, Coastal and Shelf Science 50, 27–32.
Wolanski, E., Williams, D., Spagnol, S., Chanson, H., 2004. Undular tidal bore dynamics in the Daly Estuary, Northern Australia. Estuarine, Coastal and Shelf Science 60, 629–636.